Basolateral membrane sodium-independent Cl-/HCO3- exchanger in rat inner medullary collecting duct cell.

R A Star

Research Article

Previous studies have shown that the middle third of the rat inner medullary collecting duct (IMCD-2) secretes protons despite the absence of intercalated cells, the cell thought to secrete protons in other portions of the collecting duct. A new cell, the IMCD cell, is the predominant cell in IMCD-2. The mechanism responsible for base exit in the IMCD cell was characterized by measuring cell pH of isolated perfused tubules with 2',7'-bis(carboxyethyl)-5,6-carboxyfluorescein. Reduction of bath HCO3- caused a significant and reversible decrease in cell pH, whereas a similar change in luminal HCO3- had a significantly smaller effect, indicating that the HCO3-/H+ permeability of the basolateral membrane is much larger than the apical membrane. The rate of cell acidification induced by reduction in bath HCO3-, a measure of basolateral HCO3- transport, was significantly decreased in the absence of bath and lumen Cl. Decreases in bath Cl caused a significant and reversible increase in cell pH, which was not changed significantly by complete removal of Na from perfusate and bath, but was significantly inhibited by basolateral 4',5'-diisothiocyanostilbene-2,2'-disulfonic acid. A chemical voltage clamp did not inhibit the rate of cell alkalinization after bath Cl removal, indicating that Cl-/HCO3- exchange is not via parallel Cl and HCO3- conductances. Cell pH was measured in single cells by low-light-level imaging to show that most cells contain the […]

Find the latest version:

Basolateral Membrane Sodium-independent Cl⁻/HCO₃⁻ Exchanger in Rat Inner Medullary Collecting Duct Cell

Robert A. Star

Department of Internal Medicine, University of Texas Southwestern Medical Center, Dallas, Texas 75235-8856

Abstract

Previous studies have shown that the middle third of the rat inner medullary collecting duct (IMCD-2) secretes protons despite the absence of intercalated cells, the cell thought to secrete protons in other portions of the collecting duct. A new cell, the IMCD cell, is the predominant cell in IMCD-2. The mechanism responsible for base exit in the IMCD cell was characterized by measuring cell pH of isolated perfused tubules with 2',7'-bis-(carboxyethyl)-5,6-carboxyfluorescein. Reduction of bath HCO_3^- caused a significant and reversible decrease in cell pH, whereas a similar change in luminal HCO_3^- had a significantly smaller effect, indicating that the HCO_3^-/H^+ permeability of the basolateral membrane is much larger than the apical membrane. The rate of cell acidification induced by reduction in bath HCO_3^-, a measure of basolateral HCO_3^- transport, was significantly decreased in the absence of bath and lumen Cl. Decreases in bath Cl caused a significant and reversible increase in cell pH, which was not changed significantly by complete removal of Na from perfusate and bath, but was significantly inhibited by basolateral 4',5'-diisothiocyanostilbene-2,2'-disulfonic acid. A chemical voltage clamp did not inhibit the rate of cell alkalinization after bath Cl removal, indicating that Cl⁻/HCO_3^- exchange is not via parallel Cl and HCO_3^- conductances. Cell pH was measured in single cells by low-light-level imaging to show that most cells contain the chloride-dependent HCO_3^- pathway. We conclude that the rat IMCD cell possesses a basolateral Na-independent Cl⁻/HCO_3^- exchanger which may serve as the base exit step for transepithelial proton secretion. (*J. Clin. Invest.* 1990. 85:1959–1966.) anion exchanger • 2',7'-bis-(carboxyethyl)-5,6-carboxyfluorescein (BCECF) • cell pH

Introduction

The inner medullary collecting duct (IMCD)[1] absorbs HCO_3^-, secretes ammonia, and titrates luminal buffers (1–6). How-

---

---

1. *Abbreviations used in this paper:* BCECF, 2',7'-bis-(carboxyethyl)-5,6-carboxyfluorescein; BCECF-AM, BCECF acetoxymethyl ester;

---

ever, there are both morphologic (7, 8) and functional differences (9, 10) along the IMCD. Alpha intercalated cells, the cell type generally thought to be involved in proton transport in the remainder of the collecting duct system, constitute 10% of the cells in the first third (IMCD-1) of the rat IMCD, but are absent from the second (IMCD-2) and third (IMCD-3) portions of the IMCD (11, 12). Principal cells, which are morphologically similar to principal cells found in the cortical and outer medullary collecting duct (with a central cilium), are present in IMCD-1 and in the early portion of IMCD-2 (7, 8). A newly described IMCD cell, which lacks an apical cilium, is first found in the early IMCD-2, and comprises almost all of the distal IMCD-2 and the entire IMCD-3 (7, 8).

A recent in vitro microperfusion study of the rat IMCD-2 has demonstrated luminal acidification, HCO_3^- absorption, and ammonia secretion (12). Since alpha intercalated cells are absent from the IMCD-2, this suggests that some other cell type can secrete protons. The cellular mechanism of transepithelial proton secretion in the rat IMCD-2 is unknown. In intercalated cells in other portions of the collecting duct, protons are secreted by an apical membrane H^+-ATPase while base exits via a Cl⁻/HCO_3^- exchanger on the basolateral membrane (13–16). In the IMCD, many studies have found evidence compatible with a H^+-ATPase (3, 17–20). A Cl⁻/HCO_3^- exchanger has been postulated based on stilbene-sensitive HCO_3^- absorption (3), and changes in cell pH in cells cultured from the inner medulla (20, 21). However, antibodies directed against the erythrocyte band-3 Cl⁻/HCO_3^- exchanger have not stained rabbit or rat IMCD-2 (7, 22). Furthermore, previous studies could not localize the functional activity to the apical or basolateral membrane.

The purpose of these studies was to determine the mechanism of base exit in the distal portion of the rat IMCD-2. By using the in vitro isolated tubule preparation, we could study transport across the basolateral membrane in a well defined area of the tubule containing IMCD cells.

Methods

IMCD from kidneys of pathogen-free Sprague-Dawley rats (Harlan Sprague Dawley, Inc., Indianapolis, IN) were isolated and perfused in vitro using previously described techniques (23). Rats were given a 3% body weight i.p. injection of 2.5% dextrose, allowing the tubules to be placed in isotonic dissection media without danger of osmotic shock (9, 23). Tubules were dissected at 17° in solution 1 (Table I). The tubule segments were dissected from the middle third of the inner medulla; the distal end of the tubule was at the junction between IMCD-2 and IMCD-3. Because of the short perfused length of the tubules (200–400 µm), all tubules came from the distal IMCD-2 (corresponding to 50–66% of the length of the inner medulla). The dissected tubules were mounted on pipettes for in vitro microperfusion at

---

DIC, differential interference contrast; DIDS, 4',5'-diisothiocyanostilbene-2,2'-disulphonic acid; IMCD, inner medullary collecting duct; NMDG, *N*-methyl-D-glucamine; VAL, valinomycin.

Table I. Composition of Solutions

	1	2	3	4	5	6	7	8
				mM				
NaCl	120	120						
Na gluconate		20	120	140				
NMDG Cl					120			
NMDG-gluconate						120		
KCl							120	
K gluconate								120
NaHCO₃	25	5	25	5				
NMDG-HCO₃					25	25		
CaCl₂	2	2.8			2		2	
Ca gluconate			14	14		14		14
Hepes		25						

In addition, all solutions contained glucose 5 mM, K_2HPO_4 2 mM, and $MgSO_4$ 1.2 mM.

37°C using methods of Burg (24). Perfused tubules were mounted in a laminar flow bath chamber with a volume of $\sim$ 70 μl which facilitated rapid exchanges of bathing solution (25). The bath chamber was blackened to minimize light scattering. The perfusate and bathing systems were designed to allow rapid changes between several fluids. The bath solution was continually exchanged at 5–7 ml/min by hydrostatic pressure; the luminal perfusion rate was > 20 nl/min. To minimize fluid transients in the bath chamber during a bath exchange, the bath solution was switched by computer-driven miniature pinch valves (Angar Scientific Co., Inc., Cedar Knolls, NJ). The bath solution could be 95% exchanged within 1 s as measured by appearance of blue dye or fluorescent 2',7'-bis-(carboxyethyl)-5,6-carboxyfluorescein (BCECF) acid.

In experiments requiring rapid luminal exchanges, a hydraulic arrangement was devised. Two pieces of glass tubing (0.45 mm o.d.) inserted into the back of the inner perfusion pipette carried two perfusate solutions to the tip of the perfusion pipette. Computer-driven valves controlled which of the two solutions were driven to the tip of the perfusion pipette. During fluid exchanges, the fluid at the tip of the perfusion pipette was exchanged at 1 ml/min allowing the perfusate solution to be 95% exchanged within 1 s without significant movement of the tubule.

The cell pH was measured with the trapped intracellular pH probe BCECF (26). After a 15-min equilibration period, the background autofluorescence was measured, and tubules were then loaded with 2.2 μM BCECF-acetoxymethyl ester (BCECF-AM, Molecular Probes, Inc., Eugene, OR) for 5–10 min using the method of Thomas et al. (27). After BCECF-AM was washed out of the bath chamber, the tubules were equilibrated for an additional 10 min to stabilize the intracellular concentration of BCECF, and to dissipate the acid and formaldehyde load imposed during hydrolysis of the ester groups. Fluorescence of intracellular BCECF at the end of each experimental protocol (at 440 nm) was at least 15–20 times the background autofluorescence of the tubule ($n = 8$) and the fluorescence decayed at a rate of 0.42±0.004% per min ($n = 5$), permitting sufficient time to make measurements.

The fluorescence of BCECF was measured at 530 nm with a photomultiplier tube during alternate excitation at 440 and 500 nm (26). Excitation filters were changed manually. Measurements were made with an oil inversion objective (Neofluar ×63/1.25 NA, Carl Zeiss, Inc., Thornwood, NY). An adjustable measuring box limited the measurement of fluorescence to a tubule section of $\sim$ 60 μm in length. To minimize photodamage, the intensity of the excitation light was reduced $\sim$ 200-fold with neutral density filters, the exposure time was minimized with an electronic shutter, and all solutions were bubbled

with 94% air. Background autofluorescence of the tubule and optical system was determined before loading each tubule with BCECF; all measurements were corrected for background autofluorescence. All ion substitutions and drugs added to the bathing solutions did not change the background autofluorescence. The continuous-flow bath exchange system prevented dye that may have leaked out of the cell from contributing to the measured fluorescence. The pH-dependent shift in excitation spectrum of BCECF was quantitated using an intensity ratio method (26), providing a measurement that is unaffected by changes in dye concentration, bleaching or leakage.

Fluorescence excitation ratios were converted to apparent pH values by using the calibration technique of Thomas et al. (27). Tubules were perfused and bathed with well-buffered solutions (25 mM Hepes, 60 mM phosphate) at various pH values (8.0, 7.6, 7.1, 6.6) containing nigericin (10 mg/ml) and 120 mM K^+. This K^+ concentration was chosen to approximate the intracellular K^+ concentration measured at the tip of the rat IMCD by electron microprobe analysis during furosemide-induced diuresis (28). Fig. 1 shows a typical calibration curve of BCECF determined in seven tubules.

In some studies the initial rate of change of cell pH was measured following the solution change. Since the fluorescence at the 440-nm excitation is unaffected by cell pH (26), and changes very slowly with time, changes in cell pH can be calculated as follows: $d(pH)/dt = d(pH)/d(ratio) \times [d(F_{500})/dt]/F_{440}$, where $d(pH)/d(ratio)$ is obtained from the slope of the calibration curve, $[d(F_{500}/dt)]$ is the slope of the line drawn tangent to the initial deflection, and F_{440} is obtained by interpolation between 440-nm excitation measurements made just before and after the solution change (26). In some protocols, cell pH changed slowly enough for direct measurement as $\Delta pH/\Delta$ time.

Imaging studies. In some studies, tubules were observed by video-enhanced differential interference contrast (DIC) microscopy (25) using a ×63 oil immersion objective (Zeiss Neofluor 1.25 NA) and a ×32 objective condenser lens (0.40 NA, E. Leitz, Rockleigh, NJ). Images of the lateral tubule wall were recorded by a television camera (model 65, Dage-MTI, Inc., Michigan City, IN) coupled to a super VHS video tape recorder (model HR-8000U, JVC, Elmwood Park, NJ). The final image was viewed on a TV monitor (PVM-1271Q, Sony, Park Ridge, NJ) at a final magnification of $\approx$ ×3,500.

In some studies, single cell pH was measured by low light level imaging. 8–10 cells on the lateral tubule wall were first located using DIC optics. BCECF fluorescence in individual cells was detected by an image intensifier (model KS-1380, VideoScope; Washington, DC) coupled to an television camera and passed to an image processor (Series 151, Imaging Technology, Woburn, MA). A long-pass barrier filter was used (LG530, Corion Corp., Holliston, MA). The signal-to-noise ratio of the video image was improved by summation of 16 video frames. All images were corrected by a similarly obtained dark current image, and smoothed using a center-weighted 3 × 3 kernel before storage on disk. Image pairs, consisting of images taken with sequential
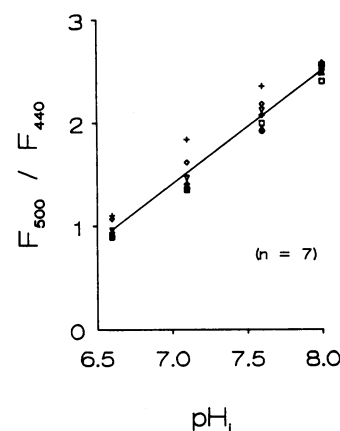

Figure 1. Intracellular calibration curve for BCECF in rat IMCD-2 tubules. Tubules were loaded with 2.2 μM BCECF-AM for 5–10 min at 37°C. Intracellular pH clamped at pH 6.6, 7.1, 7.6, and 8.0. using nigericin (10 mg/ml) and 120 mM K^+ (27). Slope was 1.1 ratio unit/pH unit.

illumination with 440- and 500-nm light, could be obtained every 15 s. After an equilibration period of 30–40 min, a DIC image was recorded, and then a fluorescent image pair was recorded. The bath solution was switched, and image pairs were recorded every 15–30 s for 2–3 min. The bath solution was switched back to the original solution, and more fluorescent image pairs were taken. At the end of the experiment, a DIC image was taken to ensure that the tubule had not moved during the bath switch.

Statistics. All results are reported as mean±1 SE. Statistical significance was determined using *t* tests (paired and nonpaired). $P < 0.05$ was considered statistically significant.

Results

Cell morphology. Previous studies have shown that the distal portion of the rat IMCD-2 consists of a single cell type, the IMCD cell [7, 8]. We found that the epithelium was composed of a single cell type which had a hexagonal apical profile, very bland intracellular composition, a quite characteristic nucleus containing a central nucleolus, and lacking a cilium on the apical membrane (Fig. 2 *A*). These IMCD cells were easily differentiated from intercalated cells (round apical profile, apical bulging into the lumen, and numerous intracellular organelles [29]) or principal cells (slightly more complex intra-

cellular cytoplasm with a characteristic single cilium on the apical membrane cell membrane [7, 8, 29]) (Fig. 2 *B*).

Effect of basolateral and luminal HCO_3^- and pH on cell pH. Perfusate and bath were perfused with solutions containing 25 mM HCO_3^- (pH 7.4, solution 1, Table I); then, either lumen or bath HCO_3^- concentration was decreased transiently to 5 mM (pH 6.8, solution 2, Table I). Fig. 3 shows a tracing from a typical study. Reduction in bath HCO_3^- concentration resulted in a marked transient decrease in the F_{500} recording, while similar change in luminal HCO_3^- caused very little decrease in F_{500}. In the third period, reduction in bath HCO_3^- caused a transient decrease in F_{500}. In seven tubules, a fivefold reduction in bath HCO_3^- resulted in significant cell acidification from pH 7.22±0.02 to 6.92±0.04, which was reversible upon return of bath HCO_3^- to 25 mM (Fig. 3). A similar reduction in perfusate HCO_3^- caused a small but significant decrease in cell pH from 7.16±0.03 to 7.15±0.03 which was reversible to 7.16±0.03 upon restoration of luminal HCO_3^- to 25 mM. The change in cell pH caused by reduction of bath HCO_3^- was significantly greater than that caused by a reduction in luminal HCO_3^-, indicating that cell pH is more sensitive to bath HCO_3^-/H^+.

The initial rate of change in cell pH was used to determine the rate of apical and basolateral membrane HCO_3^-/H^+ trans-
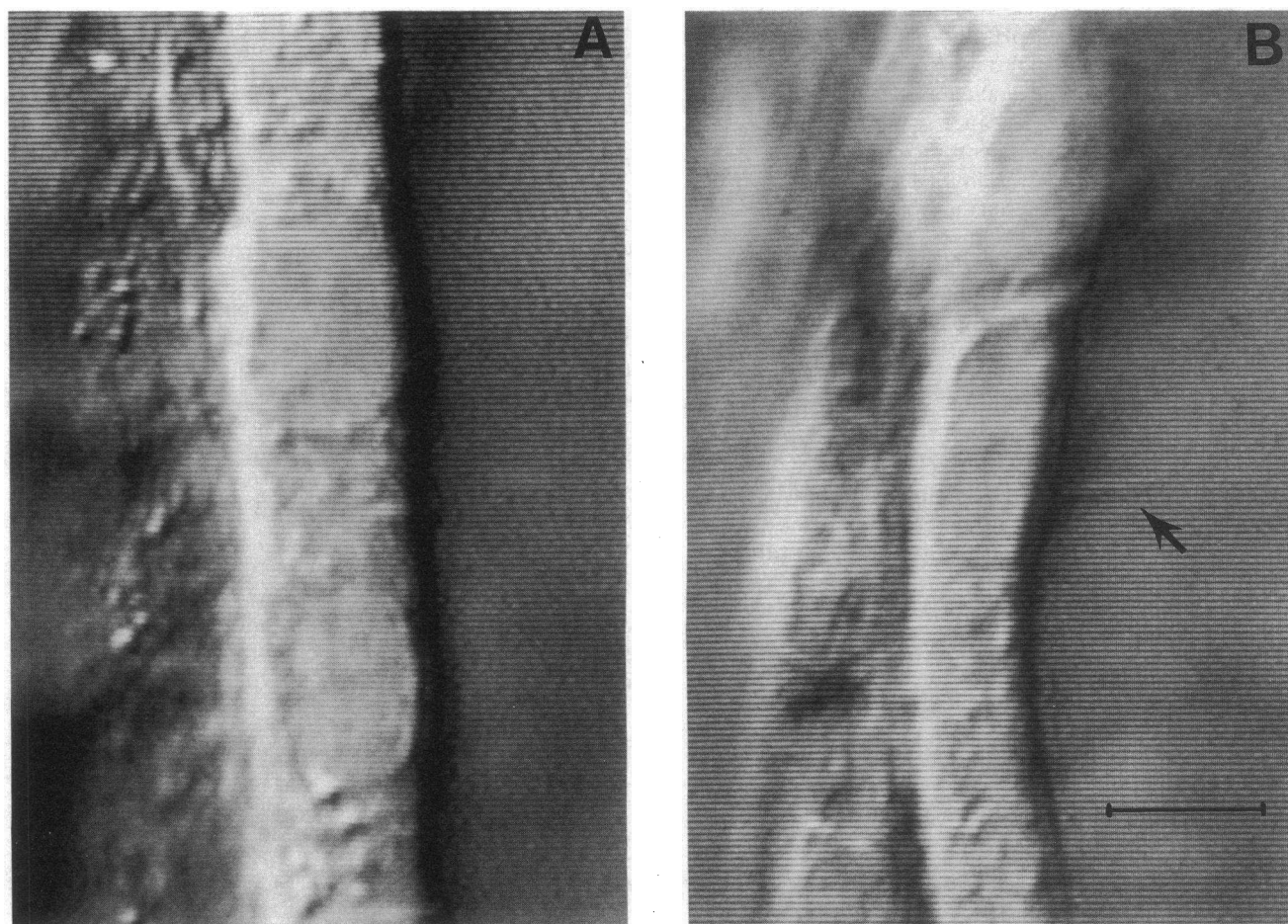

Figure 2. Images of two IMCD cells from (*A*) IMCD-2 and a principal cell from (*B*) IMCD-1. Cells imaged on the lateral tubule wall using video-enhanced DIC microscopy. The apical cell membrane is on right side of both pictures. An apical cilium is seen on principal cell (*arrow*) but not on the IMCD cell. Bar, 5 μm.
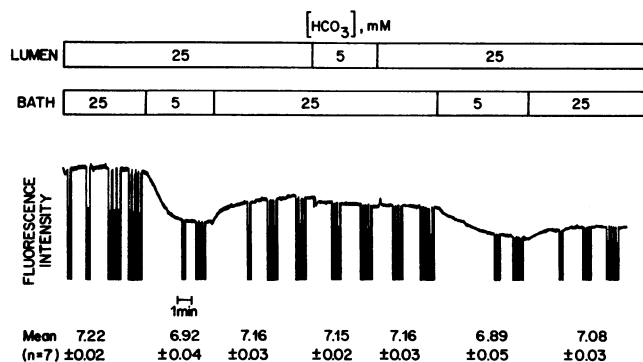
Figure 3. Typical tracing from experiment showing effect of reduction in HCO_3^- from 25 to 5 mM sequentially in bath, lumen, and bath on cell pH. Fluorescence emission intensity was measured at excitation 450-nm excitation (*smooth curve*) and 500-nm excitation (*interrupted portion*). HCO_3 was replaced with gluconate. Values at the bottom of the figure are means±SE for seven tubules.

Figure 4. Rate of cell acidification (*hatched bars*) and cell alkalinization (*open bars*) after changes in HCO_3^- sequentially in bath, lumen, and bath. Each bar represents mean±SE for seven tubules. *Statistically significant difference lumen vs. bath by paired t test.

port (Fig. 4).[2] The rate of cell acidification was significantly slower upon reduction in luminal HCO_3^- (0.02 ± 0.02 pH units min^{-1}) than upon reduction in bath HCO_3^- (0.44 ± 0.11 pH units min^{-1}), suggesting that the HCO_3^-/H^+ permeability is larger in the basolateral membrane than the apical membrane.[3] Because this basolateral membrane pathway is more important in control of cell pH, and has a larger HCO_3^-/H^+ permeability, subsequent studies were carried out to examine the mechanism of this basolateral pathway.

Effect of bath Cl^- removal. Since many of the previously described distal nephron basolateral membrane HCO_3^- transporters are coupled to Cl^-, we examined the effect of bath Cl^- removal on cell pH. A typical tracing is shown in Fig. 5. In 10 tubules, removal of bath Cl^- (solution 3, Table I) significantly alkalinized the cell from pH 7.17 ± 0.03 to 7.55 ± 0.03. In most tubules, this was followed by a significant acidification of cell pH by -0.10 ± 0.03 pH units which returned cell pH back towards normal.[4] Restoration of bath Cl^- resulted in a rapid acidification of the cell to 7.06 ± 0.3, which is significantly below the starting cell pH. These results suggest that HCO_3^- transport is coupled to Cl^-.

Cl^- dependence of basolateral HCO_3^- pathway. The Cl^- and HCO_3^- fluxes could be coupled either directly via an exchanger or indirectly via changes in transmembrane voltage. For example, the effect of bath Cl^- removal on cell pH could be explained by a Cl^- conductance in parallel with either a basolateral membrane HCO_3^- conductance or a voltage-sensi-
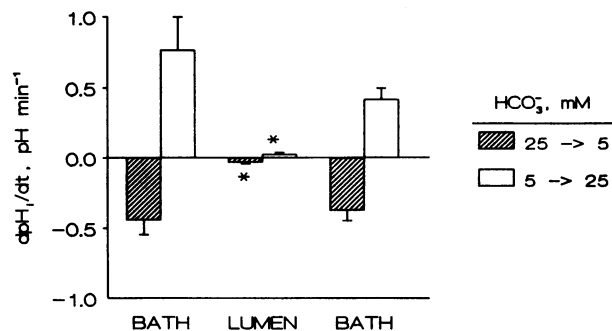
tive H^+-ATPase. Removal of external Cl^- would depolarize the cell, which in turn could either stimulate a H^+-ATPase or allow HCO_3^- entrance through a parallel HCO_3^- conductance, both leading to cell alkalinization. We used two protocols to differentiate between direct and indirect coupling.

First, the Cl^- dependence of the basolateral pathway was studied since the apparent HCO_3^- permeability would be Cl^- dependent only with a directly coupled exchanger. The change in cell pH in response to a decrease in bath HCO_3^- from 25 to 5 mM was studied sequentially in the presence, absence, and presence of Cl^-. In the presence of bath and lumen Cl^- (solution 1, Table I), a reduction in bath HCO_3^- from 25 to 5 mM (solution 2, Table I) resulted in a cell acidification from pH 7.26 ± 0.02 to 7.15 ± 0.04 which returned to control pH ($7.26\pm.02$) upon return of bath HCO_3^- to 25 mM. Removal of both lumen and bath Cl^- (solution 3, Table I) for 5 min resulted in alkalinization of the cell to pH 7.33 ± 0.05. In the absence of Cl^-, a similar reduction in bath HCO_3^- (solution 4, Table I) caused cell pH to decline from 7.33 ± 0.05 to 7.26 ± 0.07 which was partially reversible. The change in cell pH in the absence of Cl^- was significantly less than in its presence. Restoration of Cl^- to the bath luminal solutions resulted in cell acidification to pH 7.11 ± 0.04. Fig. 6 shows the initial rate of change of cell pH caused a decrease in bath HCO_3^- concentration from 25 to 5 mM (*hatched bars*), and subsequent return to 25 mM (*open bars*). In the absence of bath and lumen Cl^- (second period), the initial rate of cell acidification was reduced significantly by $73\pm4\%$, and the initial rate of cell alkalinization was reduced significantly by $73\pm9\%$.[5] The inhibition by Cl^- removal was reversed by re-addition of Cl^- to lumen and bath (third period, Fig. 6). These results indicate that approximately three-quarters of the basolateral HCO_3^- pathway is coupled to Cl^-.

Effect of chemical voltage clamp. To further rule out indirect coupling via changes in transmembrane voltage, we volt-

2. The terms base and HCO_3^- will be used interchangeably; we recognize, however, that these studies cannot distinguish between transport of OH^- or HCO_3^-.

3. It is possible that the minimal effects of luminal pH on cell pH could be due to the stabilization of cell pH by basolateral transport mechanisms rather than the differences in membrane HCO_3^- permeability as in the rat proximal convoluted tubule (30).

4. Although the mechanism for this late acidification was not studied in this report, it appears to be sodium dependent since the late acidification was not seen after 5 min of sodium removal (unpublished observations). It is merely noted because of its ability to restore cell pH towards normal which will be used in a later protocol in the paper. A similar late acidification was found in gastric parietal cells and avian osteoclasts (31, 32) and was inhibited by dimethyl amiloride (31).

5. Because of concern that the alkaline cell pH found in the absence of bath and lumen Cl^- might inhibit the basolateral HCO_3^- pathway (although cell alkalinization stimulates Cl^-/HCO_3^- exchange [20, 33]) or change the intracellular buffer capacity, cell pH was reset towards normal by exposing tubules to Cl^--free bath and lumen solutions for 10–15 min (see Fig. 4). Under these conditions, Cl^- removal still reduced the extent of change in cell pH after a reduction in bath HCO_3^-, and also significantly inhibited the initial rate of change in cell pH by $67\pm12\%$.
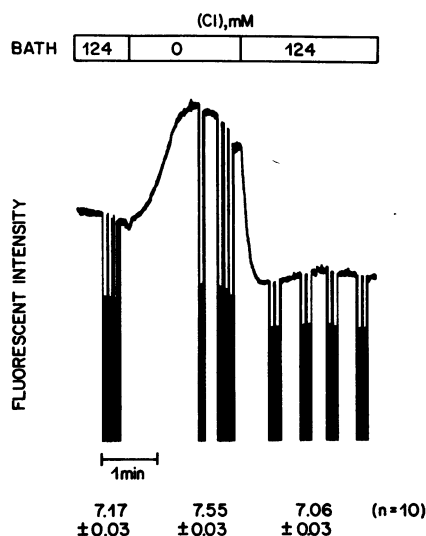
(Cl),mM

BATH | 124 | 0 | 124 |

FLUORESCENT INTENSITY

├─1min─┤

7.17   7.55   7.06   (n=10)
±0.03   ±0.03   ±0.03

Figure 5. Typical tracing from experiment showing effect of bath Cl⁻ removal on cell pH. Cl⁻ was replaced with gluconate.

age clamped the membrane with the K-ionophore valinomycin (VAL) (10 μM) and potassium (120 mM) (solution 7, Table I) (16) which was used for both bath and perfusate. Addition of valinomycin and high potassium to bath and perfusate did cause a small but not statistically significant increase in cell pH (from 7.09±0.03 to 7.12±0.02). The chemical voltage clamp increased the extent of cell alkalinization after removal of bath chloride (ΔpH: control 0.35±0.05; K/VAL 0.60±0.04; $P < 0.05$).[6] As shown in Fig. 7, the chemical voltage clamp did not affect the rate of cell alkalinization following removal of bath Cl⁻ (solution 8, Table I) (control: 0.85±0.30 pH min⁻¹ vs. K/VAL: 1.45±0.42; P = NS) or cell acidification after addition of bath Cl⁻ (4.44±1.11 pH min⁻¹ vs. 2.89±0.30; P = NS). Since K/VAL did not decrease the rates of cell alkalinization or acidification after changes in bath Cl, these results indicate that Cl⁻ and HCO₃⁻ fluxes are not coupled via changes in membrane potential, and hence are directly coupled via an exchanger.

Sodium dependence of basolateral Cl⁻ pathway. Because both sodium-dependent and sodium-independent Cl⁻/HCO₃⁻ exchangers have been described (34), we examined the sodium dependence of the basolateral Cl⁻ pathway. In the presence of sodium (solution 1, Table I), removal of bath Cl⁻ (solution 2, Table I) resulted in significant cell alkalinization of 0.42±0.03 pH units, at an initial rate of change in cell pH of 0.74±0.17 pH units min⁻¹. Removal of sodium from perfusate and bath solutions (solution 5, Table I) for 5 min caused cell acidification from 7.03±0.04 to 6.84±0.03. The cell acidification occurred after removal of sodium from the bath but not the lumen (data not shown).[7] After 5 min in sodium-free solutions, removal of basolateral Cl⁻ (solution 6, Table I) resulted

---

6. The increase in the extent of cell alkalinization, also seen in similar studies of the rabbit inner stripe collecting duct (16), may be caused by an increase in cell chloride following cell depolarization (16).

7. This may represent a basolateral Na/H antiporter which has been found by others (18–20, 35–37). The present studies would localize the transporter to the basolateral membrane where it is unlikely to mediate proton secretion but may be important for volume regulation.
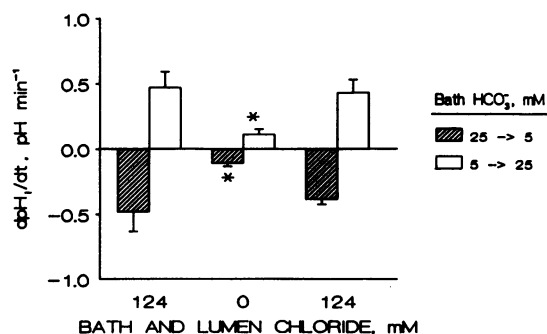

Figure 6. Effect of Cl⁻ removal on rate of cell acidification (*hatched bars*) and cell alkalinization (*open bars*) after changes in bath HCO₃⁻ concentration. *Statistically significant difference 0 mM Cl⁻ vs. 124 mM Cl⁻ by paired t test (n = 5).

in significant cell alkalinization from pH 6.84±0.03 to 7.36±0.03. The extent of cell alkalinization in the presence and absence of sodium was not significantly different. Sodium removal did not significantly effect the initial rate of cell alkalinization after removal of bath Cl⁻ or cell acidification following readdition of bath Cl⁻ (Fig. 8). Readdition of sodium to perfusate and bath restored the extent and initial rates of cell alkalinization and acidification back to control levels. These results indicate that most of the basolateral pathway is independent of sodium.

Effect of 4′,5′-diisothiocyanostilbene-2,2′-disulfonic acid (DIDS). Stilbenes inhibit sodium independent Cl⁻/HCO₃ exchangers in the rat outer medullary collecting duct (16, 38). In preliminary experiments, we found that 0.1 mM DIDS added to the bath solution caused a progressive cell acidification, so subsequent tubules were studied within 1–2 min of addition DIDS. DIDS acidified cell pH (7.09±0.03 to 7.01±0.04) within 1–2 min. DIDS significantly inhibited both the extent of cell acidification (ΔpH: control 0.36±0.03 vs. DIDS 0.09±0.02) and the rate of cell acidification in response to bath Cl⁻ removal (0.75±0.17 vs. 0.23±0.07 pH units min⁻¹) (Fig. 9).

Imaging study. While a recent study has shown that intercalated cells are absent in IMCD-2, we were concerned that only some of the cells contained a Cl⁻/HCO₃⁻ exchanger. To
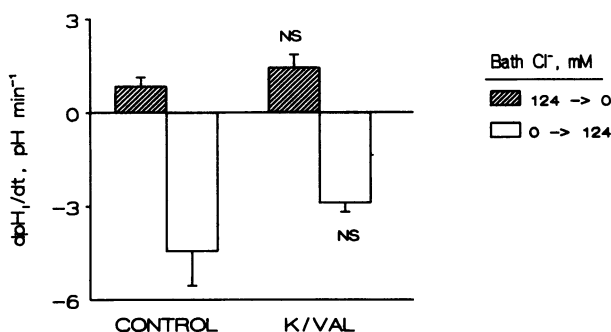

Figure 7. Effect of chemical voltage clamp (10 μM VAL and 120 mM K⁺) on the rate of cell alkalinization (*hatched bars*) and cell acidification (*open bars*) after changes in bath Cl⁻ concentration. There was no statistically significant difference in either the rate of cell acidification or the rate of cell alkalinization for K/VAL vs. control (n = 5).
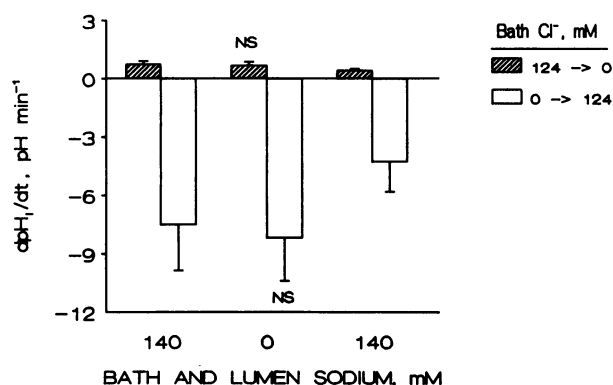
Figure 8. Effect of sodium removal on rate of cell alkalinization (hatched bars) and cell acidification (open bars) after changes in bath Cl⁻ concentration. Sodium replaced with NMDG. There was no statistically significant difference in either the rate of cell acidification or the rate of cell alkalinization for 0 vs. 140 mM Na (n = 5).

determine if the Cl⁻/HCO₃⁻ exchanger was present on only a small population of cells, cell pH was measured in 37 individual cells from four tubules. Fig. 10 shows the frequency distribution of the change in excitation ratio caused by bath Cl⁻ removal (open bars) and by restoration of bath Cl⁻ (hatched bars). The frequency distribution approximates a Gaussian curve, indicating that most of the cells contain a Cl⁻-dependent HCO₃⁻ pathway on the basolateral membrane.

Discussion

The apparent HCO₃⁻/H⁺ permeability of the basolateral membrane is larger than the apical membrane. Cell pH changed nearly imperceptibly with reduction in lumen HCO₃⁻, but was much more sensitive to bath HCO₃⁻. The initial rate of change of cell pH after reduction in lumen HCO₃⁻ was only 8–10% of that after reduction of bath HCO₃⁻. Therefore, the apparent HCO₃⁻/H⁺ permeability of the basolateral membrane is larger than the apical membrane. Similar results have been found in other portions of the collecting duct system (16). Since luminal pH in this portion of the IMCD can approach 5.9 (39), the insensitivity of cell pH to luminal pH would protect cell pH from the extremes of luminal pH. Instead, cell pH would be influenced by basolateral (systemic) pH.
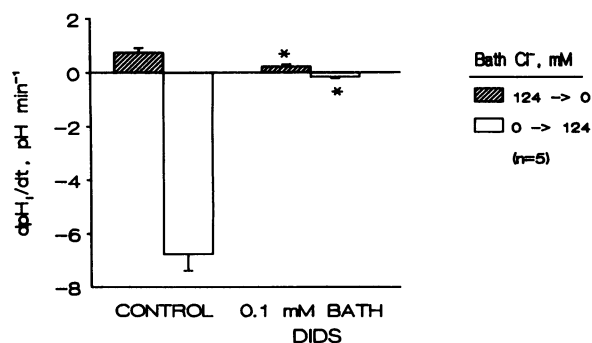

Figure 9. Effect of 0.1 mM DIDS in bath on rate of cell alkalinization (hatched bars) and cell acidification (open bars) after changes in bath Cl⁻ concentration. *Statistically significant difference DIDS vs. control by paired t test (n = 5).
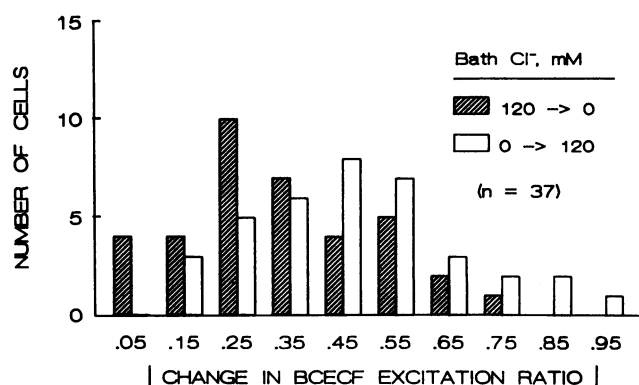

Figure 10. Frequency distribution of change in BCECF excitation ratio in individual cells after changes in bath Cl⁻ concentration. (Hatched bars) Cell alkalinization after bath Cl⁻ removal; (open bars) cell acidification after readdition of Cl⁻ to bath. Horizontal axis is expressed as absolute value of change in emission ratio so that response to bath chloride removal and readdition could be displayed on same graph. Data are from 37 cells in four tubules. Cell pH determined using low-light level imaging (see text for details).

The major pathway for basolateral membrane HCO₃⁻ transport is a DIDS-sensitive Na⁺-independent Cl⁻/HCO₃⁻ exchanger. The cell pH acidification after a reduction in bath HCO₃⁻ (Fig. 3) was largely dependent on the presence of Cl⁻ (Fig. 6), while removal of bath Cl⁻ caused cell alkalinization (Fig. 5). These findings imply that a portion of the basolateral HCO₃⁻ pathway is coupled to Cl⁻. The coupling could occur by several known mechanisms: (a) A sodium dependent Cl⁻/HCO₃⁻ exchanger is unlikely since sodium removal did not inhibit cell alkalinization following bath Cl⁻ removal (Fig. 8). (b) Tightly coupled parallel Cl⁻ and HCO₃⁻ conductances are unlikely in that removal of Cl⁻ inhibited the basolateral HCO₃⁻ permeability (Fig. 6). Furthermore, the cell depolarization by VAL plus high extracellular K⁺ also had no effect on the cell alkalinization after bath Cl⁻ removal (Fig. 7). (c) Finally, the transporter was inhibited by DIDS (Fig. 9), which inhibits Cl⁻/HCO₃⁻ exchangers and other HCO₃⁻ pathways in other tissues. Thus, the preponderance of evidence points to a Na⁺-independent Cl⁻/HCO₃⁻ exchanger.

That DIDS did not cause a detectable change in baseline cell pH might suggest that the exchanger is not active in the steady state. While DIDS alkalinizes cell pH in the inner stripe collecting duct (16), this effect is not universially present in other tissues (20, 40). Furthermore, amiloride inhibits proton secretion in the proximal convoluted tubule but does not change steady-state cell pH (41), suggesting that regulation of steady-state pH can be very complex. In addition, it is possible that our failure to detect an effect of DIDS or K/VAL on baseline cell pH may have been due to the slow rate of Cl⁻/HCO₃⁻ exchange in the absence of vasopressin, since vasopressin stimulates proton secretion in IMCD-2 (12). Therefore, the failure of DIDS to cause a measurable change in cell pH does not indicate that the Cl⁻/HCO₃⁻ exchanger is not operating under control conditions.

The studies presented do not identify the precise base which is transported, i.e., HCO₃⁻ or OH⁻ (or H⁺ in opposite direction). However, HCO₃⁻ is the predominant substrate of similar transporters in the rabbit inner stripe outer medullary collecting duct (16). We also have not studied the stoichiomet-

ric ratio, but lack of effect of the chemical voltage clamp implies that the transporter is electroneutral, and hence has a 1:1 stoichiometry, as in other tissues (42).

This study is the first to demonstrate that this transporter is in the basolateral membrane of the IMCD-2. Ullrich and Papavassiliou (3) found stilbene-sensitive HCO_3 absorption, but stilbene was present in both luminal and capillary solutions. Sun and Hebert (35) found a CO_2- and HCO_3^--dependent, DIDS-sensitive basolateral pathway mediating rapid hypertonic cell volume regulation in the rat IMCD-2; however, this pathway could not be demonstrated in the absence of vasopressin. Previous studies of cells cultured from the rat IMCD (20, 21) have detected a Cl^-/HCO_3^- exchanger, but were unable to localize the transporter to a specific membrane. In some of these studies, the origin of the tissue studied is not specified. If derived from the entire IMCD, the cells or tubules would be mostly derived from IMCD-1, given the cone shape of the inner medulla. Since intercalated cells comprise $\sim$ 10% of the cells in the IMCD-1 (11), some of the aforementioned studies may have been studying a Cl^-/HCO_3^- exchanger known to be present in the rat IMCD-1 intercalated cell by labeling with antibodies against band 3 protein (7, 43). The cellular origin(s) of the cultured cell is also not clear since the cells display functional heterogeneity (20, 44); a central apical cilium, indicative of a principal cell origin (8), is present in some studies (18) but not others (45). Intercalated cells have also been found (44).

It is surprising that antibodies directed against the erythrocyte band 3 protein anion exchanger do not label any cells in the rat or rabbit IMCD-2 (7, 22, 43), although the human IMCD-2 does label with these probes (46). The reason for the lack of staining is unknown, although a functional Cl^-/HCO_3^- exchanger which does not stain with antibodies directed against band 3 has also been found in the apical membrane of the beta intercalated cell and basolateral membrane of the principle cell of the cortical collecting duct (14, 15, 22, 47–50). Perhaps the IMCD Cl^-/HCO_3^- exchanger is also different antigenically.

Other modes of HCO_3^- exit have been described on the basolateral membrane of the rat IMCD. A basolateral HCO_3^- conductance has been found in the IMCD (51), but the tubules were taken predominantly from IMCD-1, not IMCD-2. While we did not directly probe for a HCO_3^- conductance, the lack of cell alkalinization after imposition of a chemical voltage clamp (Fig. 8), and the low apparent HCO_3^- permeability in the absence of Cl^- (Fig. 6) argue against a large HCO_3^- conductance. A Na^+-dependent Cl^-/HCO_3^- transporter has been found the proximal tubule (34); the present studies can not completely exclude its presence in the IMCD cell.

The IMCD cell contains a Cl^-/HCO_3^- exchanger. Morphological studies have demonstrated that the distal portion of IMCD-2 is composed predominantly of IMCD cells, while principal and intercalated cells are found in IMCD-1 (7, 8, 11). We were able to differentiate among these cell types using video-enhanced DIC microscopy (Fig. 2). The predominant if not exclusive cell type had a very bland cytoplasm, and lacked an apical cilium (Fig. 2 *A*), consistent with the reported features of the IMCD cell (7, 8). Although it is possible that the observed cell pH changes were confined to a few intercalated cells, we think this unlikely because (*a*) we were careful to dissect tubules from a portion of the IMCD-2 which as been shown to lack intercalated cells (7, 8, 11, 12), (*b*) dye uptake

was homogeneous (data not shown), (*c*) intercalated cells were not found in the distal IMCD-2 using video-enhanced DIC microscopy, and (*d*) most, if not all, of the cells became alkaline in response to bath Cl^- removal (Fig. 10). Therefore, the basolateral membrane Cl^-/HCO_3^- exchanger found in the current study is located in the IMCD cell.

In summary, we have found a Na^+-independent, DIDS-inhibitable Cl^-/HCO_3^- exchanger on the basolateral membrane of the rat IMCD cell. Since the rat IMCD-2 secretes protons (12), and since stilbenes inhibit transepithelial HCO_3^- absorption (3), it is likely that this exchanger may serve as the base exit step for transepithelial proton secretion.

Acknowledgments

References

1. Ullrich, K. J., H. H. Hilger, and J. D. Klumper. 1958. Sekretion von ammoniumionen in den sammelrohren der saugetierniere. *Pfluegers Arch. Gesamte Physiol. Menschen Tiere.* 267:244–250.

2. Ullrich, K. J., and F. W. Eigler. 1958. Sekretion von wasserstoffionen in den sammerlohren der saugetierniere. *Pfluegers Arch. Gesamte Physiol. Menschen Tiere.* 267:491–496.

3. Ullrich, K. J., and F. Papavassiliou. 1981. Bicarbonate reabsorption in the papillary collecting duct of rats. *Pfluegers Arch. Eur. J. Physiol.* 389:271–275.

4. Richardson, R. M. A., and R. T. Kunau, Jr. 1982. Bicarbonate reabsorption in the papillary collecting duct: effect of acetazolamide. *Am. J. Physiol.* 243:F74–F80.

5. DuBose, T. D., Jr., and C. R. Caflisch. 1988. Effect of selective aldosterone deficiency on acidification in nephron segments of the rat inner medulla. *J. Clin. Invest.* 82:1624–1632.

6. Good, D. W., C. R. Caflisch, and T. D. DuBose, Jr. 1987. Transepithelial ammonia concentration gradients in inner medulla of the rat. *Am. J. Physiol.* 252:F491–F500.

7. Madsen, K. M., W. L. Clapp, and J. W. Verlander. 1988. Structure and function of the inner medullary collecting duct. *Kidney Int.* 34:441–454.

8. Clapp, W. L., K. M. Madsen, J. W. Verlander, and C. C. Tisher. 1989. Morphologic heterogeneity along the rat inner medullary collecting duct. *Lab. Invest.* 60:219–230.

9. Sands, J. M., and M. A. Knepper. 1987. Urea permeability of mammalian inner medullary collecting duct system and papillary surface epithelium. *J. Clin. Invest.* 79:138–147.

10. Sands, J. M., H. Nonoguchi, and M. A. Knepper. 1987. Vasopressin effects on urea and H_2O transport in inner medullary collecting duct subsegments. *Am. J. Physiol.* 253:F823–F832.

11. Clapp, W. L., K. M. Madsen, J. W. Verlander, and C. C. Tisher. 1987. Intercalated cells of the rat inner medullary collecting duct. *Kidney Int.* 31:1080–1087.

12. Wall, S. M., J. M. Sands, M. F. Flessner, H. Nonoguchi, K. R. Spring, and M. A. Knepper. 1990. Net acid transport in isolated perfused rat inner medullary collecting ducts. *Am. J. Physiol.* 258:F75–F84.

13. Brown, D., S. Hirsch, and S. Gluck. 1988. Localization of a proton-pumping ATPase in rat kidney. *J. Clin. Invest.* 82:2114–2126.

14. Schuster, V. L., and S. Gluck. 1989. Co-existence of H^+-ATPase and band 3 Cl-HCO_3 exchanger in rabbit collecting duct (CD) intercalated cells. *Kidney Int.* 35:463. (Abstr.)

15. Alper, S. L., J. Natale, S. Gluck, H. F. Lodish, and D. Brown. 1989. Subtypes of intercalated cells in rat kidney collecting duct de-

fined by antibodies against erythroid band 3 and renal vacuolar H^+-ATPase. *Proc. Natl. Acad. Sci. USA.* 86:5429–5433.

16. Hays, S. R., and R. J. Alpern. 1990. Basolateral membrane Na^+-independent Cl^-/HCO_3^- exchange in the inner stripe of the rabbit outer medullary collecting tubule. *J. Gen. Physiol.* 95:347–367.

17. Garg, L. C., and N. Narang. 1985. Stimulation of an N-ethyl-maleimide-sensitive ATPase in the collecting duct segments of the rat nephron by metabolic acidosis. *Can. J. Physiol. Pharmacol.* 63:1291–1296.

18. Kleinman, J. G., S. S. Blumenthal, J. H. Wiessner, K. L. Reetz, D. L. Lewand, N. S. Mandel, G. S. Mandel, J. C. Garancis, and E. J. Cragoe, Jr. 1987. Regulation of pH in rat papillary tubule cells in primary culture. *J. Clin. Invest.* 80:1660–1669.

19. Selvaggio, A. M., J. H. Schwartz, H. H. Bengele, F. D. Gordon, and E. A. Alexander. 1988. Mechanisms of H^+ secretion by inner medullary collecting duct cells. *Am. J. Physiol.* 254:F391–F400.

20. Brion, L. P., J. H. Schwartz, H. M. Lachman, B. J. Zavilowitz, and G. J. Schwartz. 1989. Development of H^+ secretion by cultured renal inner medullary collecting duct cells. *Am. J. Physiol.* 257:F486–F501.

21. Kim, C., E. P. Nord, and J. A. Kraut. 1989. Cl^-/HCO_3^- exchange of inner medullary collecting duct (IMCD) cells is predominantly a Na^+-independent process. *Kidney Int.* 35:456. (Abstr.)

22. Schuster, V. L., S. M. Bonsib, and M. L. Jennings. 1986. Two types of collecting duct mitochondria-rich (intercalated) cells: lectin and band 3 cytochemistry. *Am. J. Physiol.* 251:C347–C355.

23. Star, R. A., H. Nonoguchi, R. Balaban, and M. A. Knepper. 1988. Calcium and cyclic adenosine monophosphate as second messengers for vasopressin in the rat inner medullary collecting duct. *J. Clin. Invest.* 81:1879–1888.

24. Burg, M. B. 1972. Perfusion of isolated renal tubules. *Yale J. Biol. Med.* 45:321–326.

25. Strange, K., and K. R. Spring. 1986. Methods for imaging renal tubule cells. *Kidney Int.* 30:192–200.

26. Alpern, R. J. 1985. Mechanism of basolateral membrane $H^+/OH^-/HCO_3^-$ transport in the rat proximal convoluted tubule. *J. Gen. Physiol.* 86:613–636.

27. Thomas, J. A., R. N. Buchsbaum, A. Zimniak, and E. Racker. 1979. Intracellular pH measurements in Ehrlich ascites tumor cells utilizing spectroscopic probes generated in situ. *Biochemistry.* 18:2210–2218.

28. Beck, F., A. Dorge, R. Rick, and K. Thurau. 1985. Osmoregulation of renal papillary cells. *Pfluegers Arch. Eur. J. Physiol.* 405(Suppl. 1):S28–S32.

29. Strange, K., and K. R. Spring. 1987. Cell membrane water permeability of rabbit cortical collecting duct. *J. Membr. Biol.* 96:27–43.

30. Alpern, R. J., and M. Chambers. 1986. Cell pH in the rat proximal convoluted tubule. Regulation by luminal and peritubular pH and sodium concentration. *J. Clin. Invest.* 78:502–510.

31. Muallem, S., D. Blissard, E. J. Cragoe, Jr., and G. Sachs. 1988. Activation of the Na^+/H^+ and Cl^-/HCO_3^- exchange by stimulation of acid secretion in the parietal cell. *J. Biol. Chem.* 263:14703–14711.

32. Teti, A., H. C. Blair, S. L. Teitelbaum, A. J. Kahn, C. Koziol, J. Konsek, A. Zambonin-Zallone, and P. H. Schlesinger. 1989. Cytoplasmic pH regulation and chloride/bicarbonate exchange in avian osteoclasts. *J. Clin. Invest.* 83:227–233.

33. Mason, M. J., J. D. Smith, J. De Jesus Garcia-Soto, and S.

Grinstein. 1989. Internal pH-sensitive site couples Cl^-/HCO_3^- exchange to Na^+-H^+ antiport in lymphocytes. *Am. J. Physiol.* 256:C428–C433.

34. Preisig, P. A., and R. J. Alpern. 1989. Basolateral membrane $H^+OH^-HCO_3^-$ transport in the proximal tubule. *Am. J. Physiol.* 256:F751–F765.

35. Sun, A., and S. C. Hebert. 1989. Rapid hypertonic cell volume regulation in the perfused inner medullary collecting duct. *Kidney Int.* 36:831–842.

36. Wall, S. M., S. Muallem, and J. A. Kraut. 1987. Detection of a Na^+-H^+ antiporter in cultured rat renal papillary collecting duct cells. *Am. J. Physiol.* 253:F889–F895.

37. Hering-Smith, K. S., I. D. Weiner, E. J. Cragoe, and L. L. Hamm. 1990. Inner medullary collecting duct (IMCD) Na^+-H^+ exchanger. *Kidney Int.* 37:538 (Abstr.)

38. Koeppen, B. M. 1989. Electrophysiology of collecting duct H^+ secretion: effect of inhibitors. *Am. J. Physiol.* 256:F79–F84.

39. Bengele, H. H., E. R. McNamara, J. H. Schwartz, and E. A. Alexander. 1988. Acidification adaptation along the inner medullary collecting duct. *Am. J. Physiol.* 255:F1155–F1159.

40. Krapf, R., R. J. Alpern, F. C. Rector, Jr., and C. A. Berry. 1987. Basolateral membrane Na/base cotransport is dependent on CO_2/HCO_3 in the proximal convoluted tubule. *J. Gen. Physiol.* 90:833–853.

41. Preisig, P. A., H. E. Ives, E. J. Cragoe, Jr., R. J. Alpern, and F. C. Rector, Jr. 1987. Role of the Na^+/H^+ antiporter in rat proximal tubule bicarbonate absorption. *J. Clin. Invest.* 80:970–978.

42. Wieth, J. O., and J. Brahm. 1985. Cellular Anion Transport. *In* The Kidney: Physiology and Pathophysiology. D. W. Seldin, and G. Giebisch, editors. Raven Press, New York. 49–90.

43. Holthofer, H., B. A. Schulte, G. Pasternack, G. J. Siegel, and S. S. Spicer. 1987. Three distinct cell populations in rat kidney collecting duct. *Am. J. Physiol.* 253:C323–C328.

44. Kleinman, J., J. Bain, D. Riley, and R. Pscheidt. 1990. Intercalated (IC) and principal (PC) cells of inner medullary collecting duct (IMCD). *Kidney Int.* 37:540. (Abstr.)

45. Husted, R. F., M. Hayashi, and J. B. Stokes. 1988. Characteristics of papillary collecting duct cells in primary culture. *Am. J. Physiol.* 255:F1160–F1169.

46. Verlander, J. W., K. M. Madsen, B. P. Croker, P. S. Low, D. P. Allen, and C. C. Tisher. 1988. Identification of a Cl^-/HCO_3^- transporter in the basolateral membrane of intercalated (IC) in the collecting duct of man. *Kidney Int.* 33:408. (Abstr.)

47. Star, R. A., M. B. Burg, and M. A. Knepper. 1985. Bicarbonate secretion and chloride absorption by rabbit cortical collecting ducts. Role of chloride/bicarbonate exchange. *J. Clin. Invest.* 76:1123–1130.

48. Verlander, J. W., K. M. Madsen, P. S. Low, D. P. Allen, and C. C. Tisher. 1988. Immunocytochemical localization of band 3 protein in the rat collecting duct. *Am. J. Physiol.* 255:F115–F125.

49. Wang, X., and I. Kurtz. 1989. Intracellular pH (pHi) regulation in the rabbit cortical collecting duct using inverted confocal fluorescence microscopy. *Clin. Res.* 37:504a. (Abstr.)

50. Schuster, V. L., and J. B. Stokes. 1987. Chloride transport by the cortical and outer medullary collecting duct. *Am. J. Physiol.* 253:F203–F212.

51. Stanton, B. A. 1989. Characterization of apical and basolateral membrane conductances of rat inner medullary collecting duct. *Am. J. Physiol.* 256:F862–F868.